REGULAR PAPER

CrossMark

Low-temperature (≥400 °C) growth of InN by metalorganic vapor phase epitaxy using an NH₃ decomposition catalyst

Akio Yamamoto[1,2]*, Kazuki Kodama[1,2], Naoteru Shigekawa[3], Takashi Matsuoka[4], and Masaaki Kuzuhara[1]

[1]University of Fukui, Fukui 910-8507, Japan
[2]JST-CREST, Kawaguchi, Saitama 332-0012, Japan
[3]Osaka City University, Osaka 558-8585, Japan
[4]IMR, Tohoku University, Sendai 980-8577, Japan

*E-mail: ayamamot@u-fukui.ac.jp

In this paper, we report the metalorganic vapor phase epitaxial (MOVPE) growth of InN using a NiO-based pellet-type NH₃ decomposition catalyst. The use of the catalyst significantly changes the growth behavior of InN, which is dependent on the growth temperature (T_g). Continuous InN films without the incorporation of metallic In and a cubic phase are grown at $T_g = 400$–480 °C. An InN film grown at $T_g \approx 450$ °C has a full-width at half maximum (FWHM) of 376 arcsec in the X-ray rocking curve for InN(0002) reflection. At $T_g \geq 500$ °C, the deposition rate of InN rapidly decreases and the deposited films become discontinuous with large (ca. 1 µm) pyramidal grains of InN. Depositions are scarcely obtained at $T_g \geq 600$ °C. Such changes in the growth behavior of InN are governed by the NH₃ decomposition. © 2016 The Japan Society of Applied Physics

1. Introduction

There has been increased interest in InN over the last 20 years because InN has the lowest effective mass, highest mobility, and highest saturation velocity among group-III nitrides.[1] The small band gap (≤ 0.7 eV) determined for InN[2] has further enhanced the interest in InN and its alloys. Intensive studies have been conducted on the growth of high-quality InN by the metalorganic vapor phase epitaxy (MOVPE) and molecular beam epitaxy (MBE) methods. Process compatibility with GaN, AlN, and their alloys and the potential for mass production have led to greater expectations for MOVPE as a method for InN growth. However, despite considerable efforts, the quality of MOVPE InN has not yet reached that of MBE samples. For example, a carrier concentration on the order of 10^{17} cm^{-3} has been realized for MBE InN,[3–5] while that of MOVPE InN remains in the mid 10^{18} cm^{-3} range.[6–8] Thus, a breakthrough has been strongly desired in MOVPE technology for the production of InN.

The optimum temperature for the MOVPE growth of InN using NH₃ was reported to be approximately 600 °C.[9] This temperature is considered to be determined by a trade-off between two major phenomena, namely the decomposition of NH₃ and the decomposition of deposited InN itself.[9] Note that the deposited InN thermally degrades when kept at 600 °C for a long time (≥ 1 h).[9] Therefore, to obtain high-quality InN by MOVPE, it is essential to enhance NH₃ decomposition at a relatively low (≤ 500 °C) temperature where no degradation of InN occurs. Also, note that lower (≤ 600 °C) temperature growth is the key to suppressing phase separation during the MOVPE growth of InN-rich thick InGaN films.[10]

We previously proposed the use of platinum group metals as NH₃ decomposition catalysts for the MOVPE of InN[11] and GaN.[12] InN films with lower carrier density and higher electron mobility were obtained using such catalysts,[11] and the carbon contamination level in GaN was markedly reduced.[12] However, the impact of catalyst use was not very marked. For example, the growth behavior properties of InN and GaN, such as the morphology and film growth rate, were not significantly affected by the use of the catalysts.
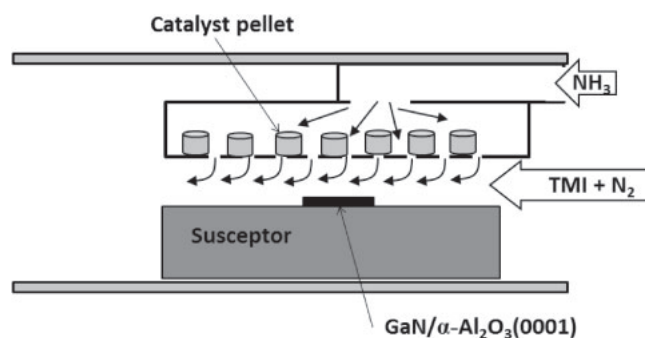
Fig. 1. Schematic diagram of the MOVPE reactor with the pellet-type NH₃ decomposition catalyst.

This is considered to be due to the very small fraction of decomposed NH₃ because of the limited surface area of the thin ($\phi 0.1$ mm × 1000 mm) catalyst wire used. In this study, we have employed NiO-based pellet-type NH₃ decomposition catalysts with a sufficiently large surface area ($\phi 17$ mm × 10 mm). Here, we investigate the growth behavior and quality of InN with the use of these catalysts.

2. Experimental procedure

The growth of InN was performed using a MOVPE system with a horizontal reactor. A Ga-polar GaN/α-Al₂O₃(0001) template was used as a substrate. Trimethylindium (TMI) and ammonia (NH₃) were used as In and N sources, respectively, and N₂ as a carrier gas. The growth temperature and pressure were varied from 400 to 600 °C and from 76 to 600 Torr, respectively. The InN growth rate was approximately 0.2 µm/h at 450 °C. Figure 1 shows a schematic drawing of the reactor design employed in this study. Pellets of the NiO-based catalyst (JGC Catalysts & Chemicals N134) were set in the catalyst chamber (150 × 150 × 15 mm³) at ca. 20 mm above the substrates in the reactor. TMI was flowed horizontally with the N₂ carrier gas, while NH₃ was introduced vertically to the substrate surface through the catalyst chamber. The catalyst pellets were radiantly heated by a radio-frequency (RF)-heated carbon susceptor. Although the temperature of the catalyst pellets was not measured, it was
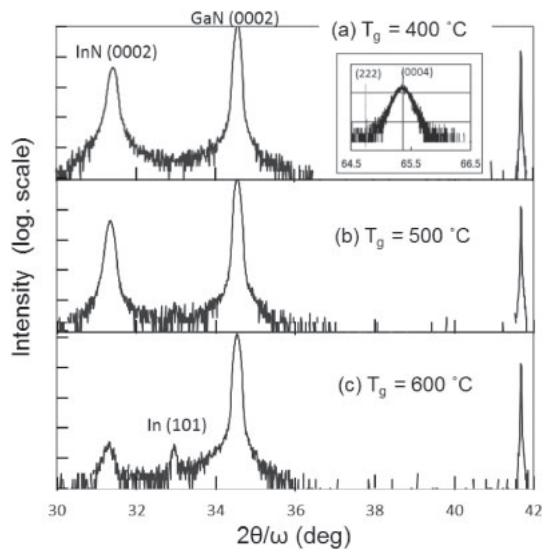
Fig. 2. HRXRD $2\theta/\omega$ patterns for samples deposited on GaN/sapphire templates at 400, 500, and 600 °C. The inset in (a) shows a magnified diffraction pattern at around $2\theta = 65.5°$, which shows no cubic (222) peak. The gas pressure during growth was 76 Torr for all samples.

assumed to be close to that of the susceptor. Deposited films were mainly characterized using high-resolution X-ray diffraction (HRXRD) and field-emission scanning electron microscopy (FESEM).

3. Results and discussion

Figure 2 shows the HRXRD $2\theta/\omega$ patterns for InN films grown at growth temperatures (T_g) from 400 to 600 °C. The

gas pressure during growth is 76 Torr for all samples. The results in Fig. 2 indicate that no materials other than InN and metallic In are deposited on the GaN/sapphire substrate. The sample deposited at 600 °C [Fig. 2(c)] shows a very weak InN(0002) peak and a relatively strong In(101) peak, which indicates that there is almost no InN growth at this temperature. This is a marked contrast from the result for the conventional MOVPE of InN, where InN growth occurs without major changes up to 650 °C.[9] Wurtzite InN films without the incorporation of metallic In were successfully obtained by a reduction in T_g down to ≤500 °C. Although cubic-phase InN was reported to grow with a decrease in T_g,[13] no cubic phase was obtained in this case even for the film deposited at $T_g = 400$ °C, as shown in the inset of Fig. 2(a). If the cubic phase is present in the film, an InN(222) peak should appear at a 2θ value 0.6° lower than that for InN(0004). Figure 3 shows the surface morphologies (FESEM micrographs) of the samples deposited at T_g from 400 to 550 °C. The gas pressure during growth was 76 Torr for all samples. The morphology of the InN film significantly changed with T_g. At T_g in the range of 400–480 °C, a continuous InN film was obtained. However, when T_g exceeded 480 °C, the deposited films became discontinuous and islands with some inclined facets were formed. In addition, grains with diameters as large as 1 µm were formed [Fig. 3(e)], despite the film thickness being approximately 0.3 µm or less, as shown later (see Fig. 4). This result is very similar to that previously reported for InN grown with a Pt catalyst heated up to 800 °C.[14] At $T_g \geq 550$ °C, the deposition on the substrate surface was not readily achieved, as shown in Fig. 3(f). Thus, an increase in T_g by only 20 °C
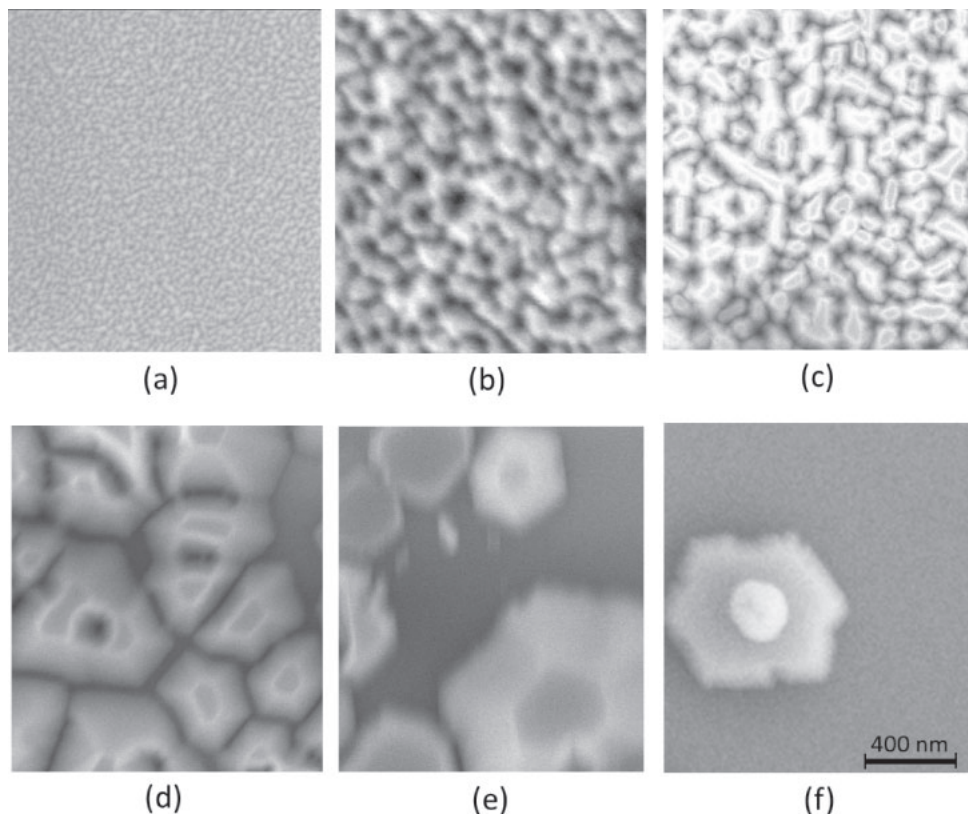
Fig. 3. Surface FESEM micrographs of samples deposited at T_g from 400 to 550 °C with the gas pressure during growth kept at 76 Torr for all samples: (a) 400, (b) 450, (c) 480, (d) 500, (e) 520, and (f) 550 °C.
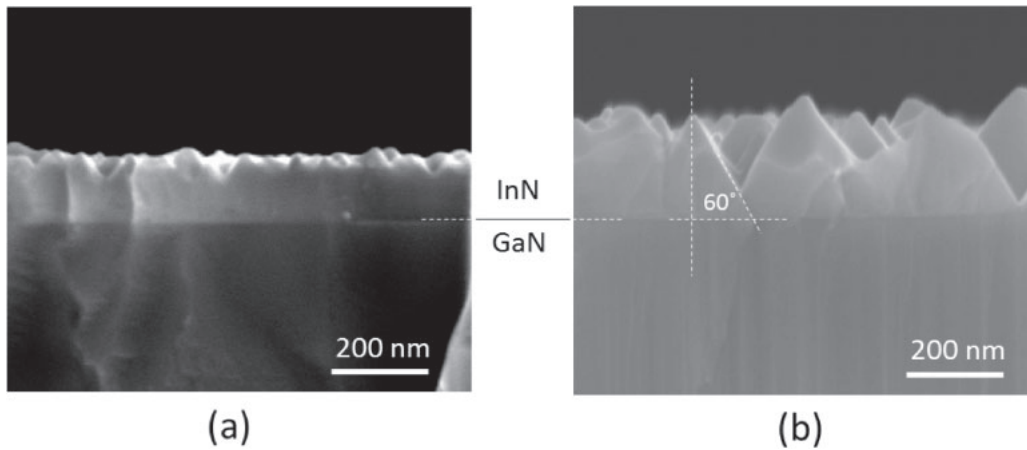
Fig. 4. Cross-sectional FESEM micrographs of samples grown at (a) 450 and (b) 500 °C with the gas pressure during growth kept at 76 Torr.
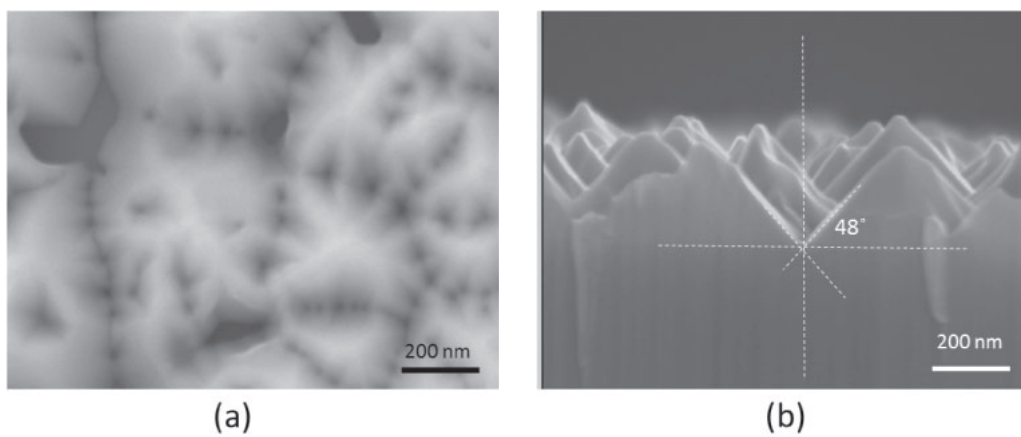
Fig. 5. (a) Surface and (b) cross-sectional FESEM micrographs of samples grown at $T_g = 500$ °C with the gas pressure at 600 Torr.

can result in significant changes in the surface morphology of the films. Figure 4 shows cross-sectional FESEM images of samples deposited at $T_g = 450$ and 500 °C with a pressure of 76 Torr. For the sample deposited at 450 °C, a continuous film with a slightly corrugated surface was obtained, while for the sample deposited at 500 °C, markedly enhanced surface corrugations and pyramidal crystal grains were formed. The angle of the sixfold inclined grain surface relative to the substrate surface is approximately 60°, as shown in Fig. 4(b). Therefore, the inclined grain surface corresponds to the $(10\bar{1}1)$ plane or close to it.[15] Figure 5 shows surface and cross-sectional FESEM images of a sample deposited at 500 °C and 600 Torr. Although the morphology of the sample is similar to that deposited at 76 Torr [Fig. 3(d)], the grains grown at 600 Torr are round and have many pits (ca. 5×10^9 cm^{-2}) at the grain boundaries, as shown in Fig. 5(a). The angle of the inclined surface of the grains is approximately 48°, as shown in Fig. 5(b). Note that the surface features shown in Figs. 3(d) and 5(a) are very similar to those of InN grown with a carrier gas containing a hydrogen species,[16] and are also similar to those of GaN films etched in a hydrogen atmosphere.[17] Therefore, it is reasonable to conclude that the appearance of the pyramidal crystal grains is related to the hydrogen etching in the growth atmosphere. Hydrogen species could be supplied by the decomposition of NH_3 in this case. The very small or zero deposition rate of InN at $T_g \geq 550$ °C is
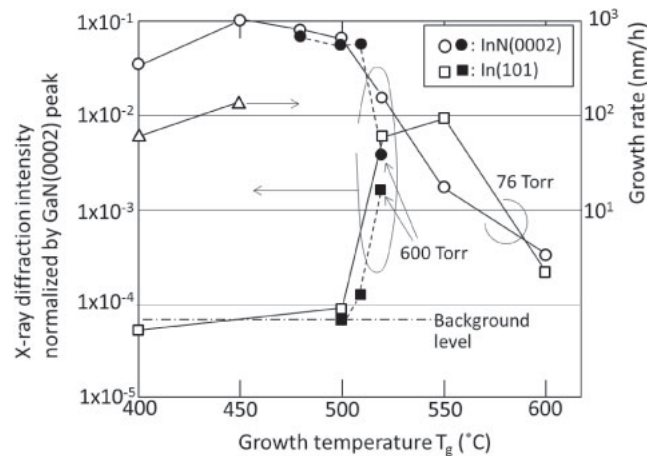
Fig. 6. HRXRD intensities of InN(0002) and metallic In(101) normalized with respect to that of GaN(0002) as a function of T_g. Growth rates of InN films grown at 400 and 450 °C are also plotted.

considered to be due to enhanced hydrogen etching, as discussed later. The formation of a high density (ca. 5×10^9 cm^{-2}) of pits in the film deposited at 600 Torr indicates that defects such as dislocations can be preferentially etched by hydrogen. Figure 6 shows the T_g dependence of the HRXRD intensity for InN(0002) and metallic In(101) normalized with respect to the underlying GaN(0002). The growth rates of the samples deposited at $T_g = 400$ and 450 °C
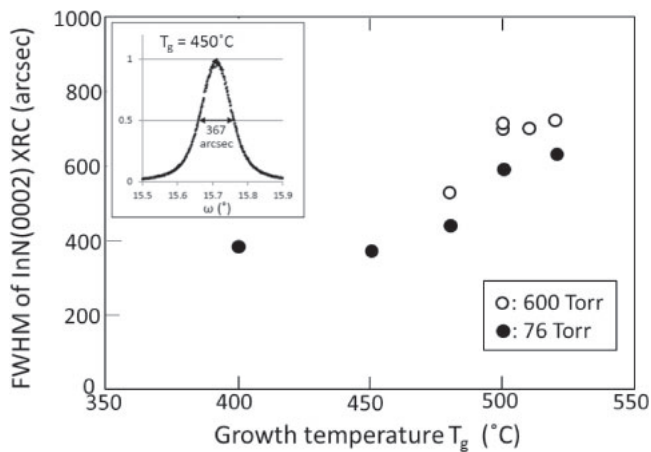
Fig. 7. Growth temperature (T_g) dependence of FWHM of the InN(0002) XRC for samples grown at 600 and 76 Torr. The inset shows a rocking curve for a sample grown at 450 °C at 76 Torr.

are also plotted in this figure. The growth rates of the samples deposited at $T_g > 480$ °C cannot be defined owing to the discontinuity of the films. The growth rates of the samples deposited at 400 and 450 °C increased with T_g. This growth rate trend corresponds to the change in the HRXRD intensity of the InN(0002) peak. Therefore, the normalized InN(0002) intensity can be used as a rough measure of the relative deposition rate of InN for the discontinuous samples. The results in Fig. 6 show that the deposition rate has a maximum at approximately $T_g = 450$ °C and then rapidly decreases as T_g increases. In accordance with the reduction in deposition rate, the intensity of In(101) significantly increases with $T_g \geq 500$ °C. Sugita et al.[14] reported that the H_2 evolution rate in the catalytic NH_3 decomposition rapidly increased when the Pt catalyst temperature exceeded 450 °C. The trend of the H_2 evolution rate is very similar to that for the decrease in deposition rate in Fig. 6. Thus, it is reasonable to consider that the hydrogen etching occurs at $T_g > 450$ °C from both the appearance of the pyramidal crystal grains (Fig. 3) and the decrease in deposition rate (Fig. 6). At $T_g \approx 600$ °C, there is almost no InN or metallic In deposition owing to the extremely enhanced hydrogen etching. This condition corresponds to the etching mode for a high H_2 mole fraction, which was thermodynamically predicted by Koukitsu et al.[18] Also, note that grains of grown InN are markedly enlarged under the conditions where hydrogen etching is marked ($T_g = 500$–550 °C). Since the enhanced grain growth is due to the enhanced migration of In atoms on the growing surface, the presence of hydrogen in the growth environment seems to contribute to the enhanced migration of In atoms.

Figure 7 shows the full-width at half maximum (FWHM) of the HRXRD rocking curve of InN(0002) as a function of T_g. An FWHM value of 376 arcsec is obtained at $T_g = 450$ °C, which is much better than those previously reported for MOVPE InN[8,16,19] and is comparable to those for MBE InN.[20–22] Such a small FWHM is believed to be due to the enhanced migration of In. Note that the increase in an FWHM at $T_g \geq 500$ °C coincides with the appearance of the isolated pyramidal crystal grains shown in Fig. 3. This indicates that a continuous film has a smaller tilt fluctuation than a discontinuous film with isolated grains. The successful growth of wurtzite InN with FWHM of ≥ 400 arcsec at $T_g =$

400–450 °C and the enhanced grain growth for samples deposited at $T_g \approx 500$ °C are due to the enhanced migration of In atoms on the growth surface, which may be related to the presence of hydrogen in the growth environment. There is a possibility that the two competitive processes, deposition and hydrogen etching, result in the enhanced migration of In. The enhanced migration of In could thus contribute to the effective suppression of cubic InN formation at $T_g \approx 400$ °C.

The electrical and optical properties of InN films grown by this method will attract much attention. A film grown at 480 °C has a carrier concentration of 1×10^{19} cm^{-3} and an electron mobility of 500 cm^2/(V·s) at room temperature. Detailed and systematic characterization is now ongoing.

Thus, the low-temperature (≥ 400 °C) MOVPE growth of InN has been performed using a NiO-based pellet-type NH_3 decomposition catalyst. An InN film with an FWHM of (0002) XRC of 376 arcsec was successfully obtained at a temperature 150 °C lower than that for conventional MOVPE (600 °C). Although further investigations are required, this technology has the potential to realize a breakthrough in the MOVPE of InN and InN-rich InGaN and InAlN.

4. Conclusions

The MOVPE growth of InN on GaN/α-Al$_2$O$_3$(0001) templates was investigated using a NiO-based pellet-type NH_3 decomposition catalyst. The growth behavior of InN is significantly influenced by the catalyst, depending on T_g. At $T_g \leq 500$ °C, wurtzite InN was successfully obtained without metallic In incorporation and no cubic phase was detected in the films deposited at 400 °C. As the best data for the FWHM of the InN(0002) XRC, a value of 376 arcsec was obtained for InN deposited at 450 °C. For $T_g \geq 450$ °C, the growth rate markedly decreased with an increase in growth temperature. There was almost no InN growth on the substrate at approximately 600 °C, in marked contrast to the conventional MOVPE. In accordance with the reduced growth rate, the grain size of the deposited InN was significantly increased and pyramidal crystal grains with diameters as large as 1 μm were grown at approximately 500 °C. The appearance of the pyramidal crystal grains and the decreased growth rate at $T_g \geq 500$ °C are due to hydrogen etching.

In a future work, the optimization of the growth conditions for InN, such as the growth temperature and pressure, will be conducted to obtain films with excellent electrical and optical properties. The secondary ion mass spectrometry (SIMS) analysis of grown films will also be performed to evaluate the presence of any contaminants from the catalyst materials.

1) A. G. Bhuiyan, A. Hashimoto, and A. Yamamoto, J. Appl. Phys. **94**, 2779 (2003).
2) V. Yu. Davydov, A. A. Klochikhin, V. V. Emtsev, S. V. Ivanov, V. V. Vekshin, F. Bechstedt, J. Furthmüller, H. Harima, A. V. Mudryi, A.

Hashimoto, A. Yamamoto, J. Aderhold, J. Graul, and E. E. Haller, Phys. Status Solidi B **230**, R4 (2002).

3) H. Lu, W. J. Schaff, L. F. Eastman, J. Wu, W. Walukiewicz, D. C. Look, and R. J. Molnar, MRS Proc. **743**, L4.10 (2002).

4) X. Wang, S.-B. Che, Y. Ishitani, and A. Yoshikawa, Jpn. J. Appl. Phys. **45**, L730 (2006).

5) F. Reurings, F. Tuomisto, C. S. Gallinat, G. Koblmüller, and J. S. Speck, Appl. Phys. Lett. **97**, 251907 (2010).

6) A. Yamamoto, H. Miwa, Y. Shibata, and A. Hashimoto, Phys. Status Solidi C **3**, 1527 (2006).

7) S. Ruffenach, M. Moret, O. Briot, and B. Gil, Phys. Status Solidi A **207**, 9 (2010).

8) L. L. Wang, H. Wang, J. Chen, X. Sun, J. J. Zhu, D. S. Jiang, H. Yang, and J. W. Liang, Superlattices Microstruct. **43**, 81 (2008).

9) A. Yamamoto, K. Sugita, and A. Hashimoto, J. Cryst. Growth **311**, 4636 (2009).

10) A. Yamamoto, T. Md Hasan, K. Kodama, N. Shigekawa, and M. Kuzuhara, J. Cryst. Growth **419**, 64 (2015).

11) K. Sasamoto, K. Sugita, A. Hashimoto, and A. Yamamoto, J. Cryst. Growth **314**, 62 (2011).

12) K. Sasamoto, T. Hotta, M. Tanaka, K. Sugita, A. G. Bhuiyan, A.

Hashimoto, and A. Yamamoto, Phys. Status Solidi C **8**, 2092 (2011).

13) T. Iwabuchi, Y. Liu, T. Kimura, Y. Zhang, K. Prasertsuk, H. Watanabe, N. Usami, R. Katayama, and T. Matsuoka, Jpn. J. Appl. Phys. **51**, 04DH02 (2012).

14) K. Sugita, D. Hironaga, A. Mihara, A. Hashimoto, and A. Yamamoto, Jpn. J. Appl. Phys. **52**, 08JD04 (2013).

15) Y. Kangawa, T. Ito, A. Koukitsu, and K. Kakimoto, Jpn. J. Appl. Phys. **53**, 100202 (2014).

16) H. Murakami, H. C. Cho, Y. Kumagai, and A. Koukitsu, J. Cryst. Growth **310**, 4954 (2008).

17) R. Kita, R. Hachiya, T. Mizutani, H. Furuhashi, and A. Kikuchi, Jpn. J. Appl. Phys. **54**, 046501 (2015).

18) A. Koukitu, T. Taki, N. Takahashi, and H. Seki, J. Cryst. Growth **197**, 99 (1999).

19) N. Dietz, M. Alevli, R. Atalay, G. Durkaya, R. Collazo, J. Tweedie, S. Mita, and Z. Sitar, Appl. Phys. Lett. **92**, 041911 (2008).

20) X. Wang, S. B. Che, Y. Ishitani, and A. Yoshikawa, Appl. Phys. Lett. **90**, 151901 (2007).

21) T. Yamaguchi and Y. Nanishi, Appl. Phys. Express **2**, 051001 (2009).

22) C. S. Gallinat, G. Koblmüller, F. Wu, and J. S. Speck, J. Appl. Phys. **107**, 053517 (2010).